IEEE Open Journal of Nanotechnology

Received 28 September 2022; revised 30 October 2022; accepted 8 November 2022. Date of publication 11 November 2022; date of current version 14 December 2022. The review of this article was arranged by Associate Editor M. Shiratani.

*Digital Object Identifier 10.1109/OJNANO.2022.3221462*

# Low-Temperature and High-Speed Fabrication of Nanocrystalline Ge Films on Cu Substrates Using Sub-Torr-Pressure Plasma Sputtering

**GIICHIRO UCHIDA, KENTA NAGAI, AYAKA WAKANA, AND YUMIKO IKEBE**

Faculty of Science and Technology, Meijo University, Nagoya 468-8502, Japan

CORRESPONDING AUTHOR: GIICHIRO UCHIDA (e-mail: uchidagi@meijo-u.ac.jp)

This work was supported by the JSPS KAKENHI under Grant 21H01076.

**ABSTRACT** We fabricated nanocrystalline Ge films using radio-frequency (RF) magnetron plasma sputtering deposition under a high Ar-gas pressure. The Ge nanograins changed from amorphous to crystalline when the distance between the Ge sputtering target and the substrate was decreased to 5 mm and the RF input power was 11.8 W/cm$^2$ (60 W), where the deposition rate was as high as 660 nm/min. In addition, the size of the nanocrystalline grains increased from 100 to 307 nm when the RF input power for plasma production was increased from 11.8 W/cm$^2$ (60 W) to 17.7 W/cm$^2$ (90 W). In the developed narrow-gap plasma process at sub-Torr pressures, nanocrystalline Ge films were successfully fabricated on Cu substrates at low temperatures, without the substrate being heated. However, when annealing was conducted under an $N_2$ atmosphere, which is the conventional method to induce solid-phase crystallization, the amorphous Ge layer on a Cu substrate changed to a $Cu_3Ge$ crystal layer through interdiffusion of Ge and Cu atoms at 400–500 °C.

**INDEX TERMS** Plasma applications, plasma control, semiconductor films, sputtering, germanium, germanium alloys.

## I. INTRODUCTION

Crystal Ge films fabricated on various substrate materials at low temperatures have versatile applications in, for example, high-capacity $Li^+$-ion batteries [1] and high-efficiency tandem solar cells [2]. Because of the limited capacity of carbon anodes in $Li^+$-ion batteries, alternative anode materials that are reactive with Li are being actively developed [3], [4]. Among these materials, Ge is one of the most interesting because it has a high theoretical capacity of 1600 mAh/g, which is much higher than the value of 372 mAh/g for a conventional carbon active material [1]. In general, the active anode layers are fabricated on Cu-foil current collectors because Cu does not react electrochemically with Li at the low operating potential of an anode. The fabrication of Ge-based $Li^+$-ion batteries requires a method that enables a Ge layer to be deposited onto a Cu substrate via a rapid and simple procedure and that also enables precise control of the Ge nanostructure to provide good stability against volume changes of the Ge anode during Li alloying/dealloying.

The metal-induced crystallization (MIC) method has been studied to realize crystalline Ge films at low temperatures [5], [6], [7], [8]. In the MIC process, a metal layer such as Al, Ag, or Au is deposited as a catalyst underneath the Ge layer and the resultant Ge/Al, Ge/Ag, or Ge/Au bilayer film is subsequently annealed at a low temperature (<400 °C) for Ge crystal growth. Also, the conventional plasma sputtering method at a low gas pressure has been reported to form a crystal Ge film, where the substrate is heated to a temperature less than 280 °C for crystallization [9], [10]. These methods require strict temperature control of the sample by annealing after film deposition and by substrate heating during deposition, which leads to a long fabrication process. In the present study, we develop an alternative method to fabricate nanocrystalline Ge films on Cu substrates in a single-step plasma sputtering process conducted at pressures in the sub-Torr range, which is two orders magnitude higher than the gas pressure used in conventional sputtering. The advantage of our process is that it enables direct fabrication of

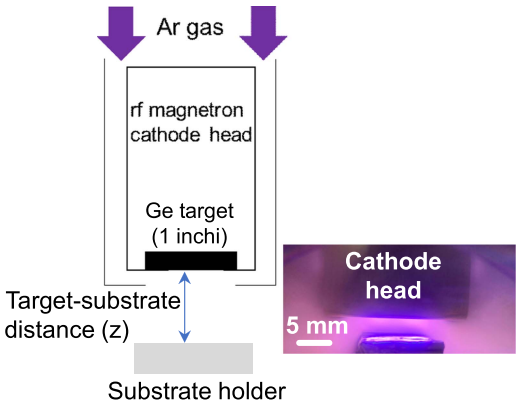


**FIGURE 1.** Schematic of the experimental setup for RF magnetron plasma sputtering and an image of the plasma emission in front of the Ge sputtering target.

nanocrystalline Ge films at high speed without heating of the substrate. The gas-phase plasma process enables control of the structure (amorphous or crystal) in the film in a simple single-step procedure [11], [12], [13].

## II. METHODS

The Ge films were fabricated on an n-type Si wafer and Cu disk using 13.56 MHz radio-frequency (RF) magnetron sputtering, as schematically shown in Fig. 1 [14]. The diameter and thickness of the Cu disk were 15 mm and 80 $\mu$m, respectively. The substrate was cleaned with ethanol using an ultrasonic cleaning bath and was then placed at the center of the substrate holder. The sputtering target was a polycrystalline Ge disk (1 inch diameter) with a purity of 99.99%. An RF power of 60 W (11.8 W/cm$^2$) was supplied to the sputtering target for plasma generation. Ar gas was supplied from the direction of the target to the substrate holder at a flow rate of 80 sccm. The Ar-gas pressure was set to a high value of 0.5 Torr. The distance between the target and the substrate holder (z) was varied from 5 to 30 mm. The substrate holder was not heated or cooled during film deposition. Some Ge films were annealed at 300–500 °C under $N_2$ for 3 h after they were deposited, where the annealing temperature was increased at a rate of 3 °C/min.

The crystal structure of the Ge films was evaluated by Raman spectroscopy (T64000, HORIBA Jobin Yvon) and X-ray diffraction (XRD) $\theta-2\theta$ scan analysis (SmartLab, Rigaku). The surface morphology and microstructure were analyzed using atomic force microscopy (AFM; Dimension FastScan, Bruker) and scanning electron microscopy (SEM; SU-8010, Hitachi).

## III. RESULTS AND DISCUSSION

Fig. 2(a), (b), and (c) show AFM surface images of Ge films deposited at target–substrate distances z of 5, 10, and 20 mm, respectively. The nanostructure of the Ge is clearly observed for all the films fabricated under a high Ar gas pressure of

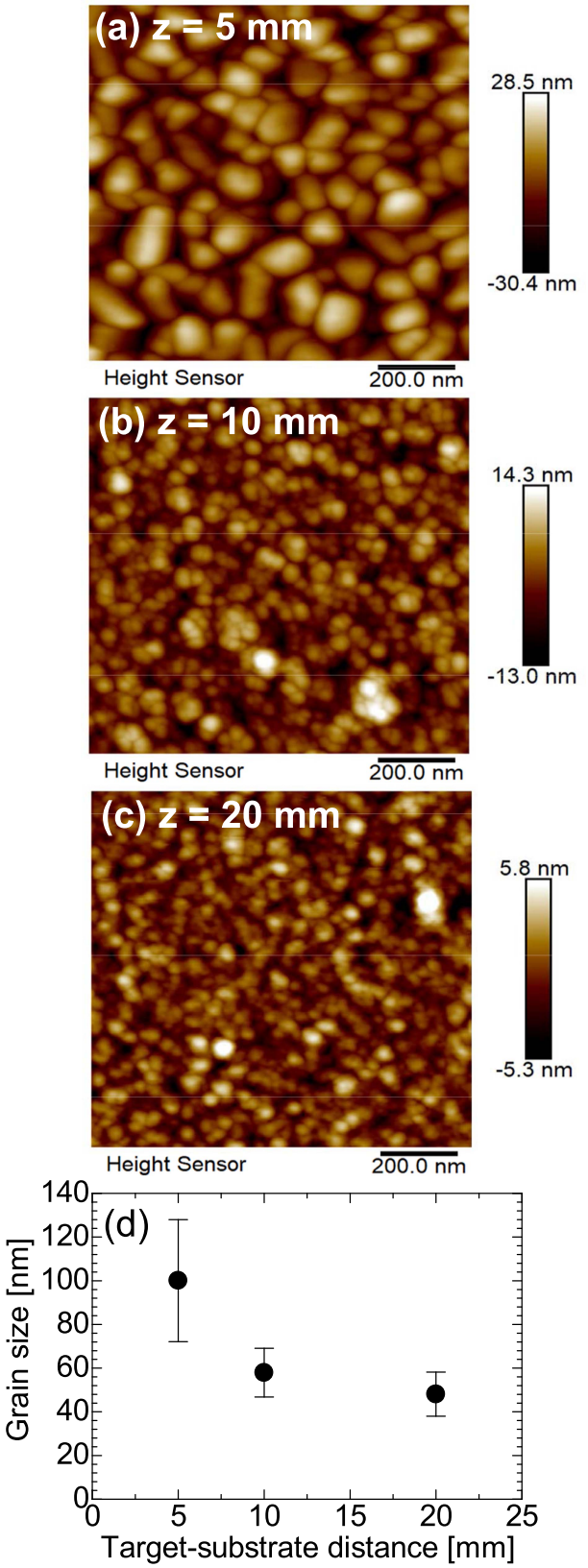


**FIGURE 2.** AFM surface images for Ge films deposited at a target–Si substrate distance z of (a) 5 mm, (b) 10 mm, and (c) 20 mm and at an RF input power of 60 W. (d) Dependence of the grain size on a target-substrate distance z.

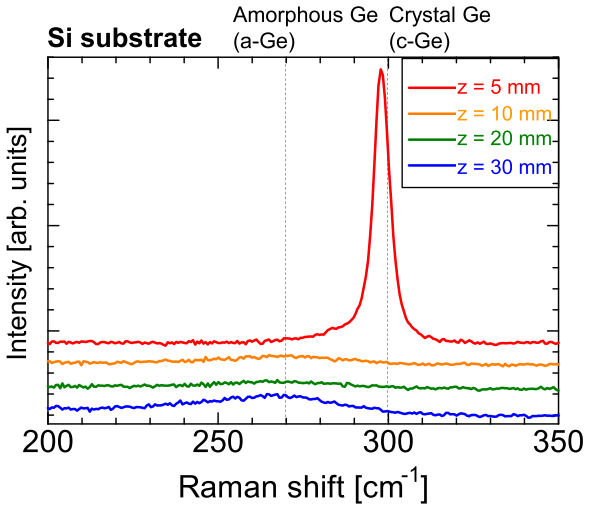


**FIGURE 3.** Raman spectrum of Ge films deposited onto Si substrates at a target–substrate distance z of 5 mm, 10 mm, 20 mm, and 30 mm and at an RF input power of 60 W.

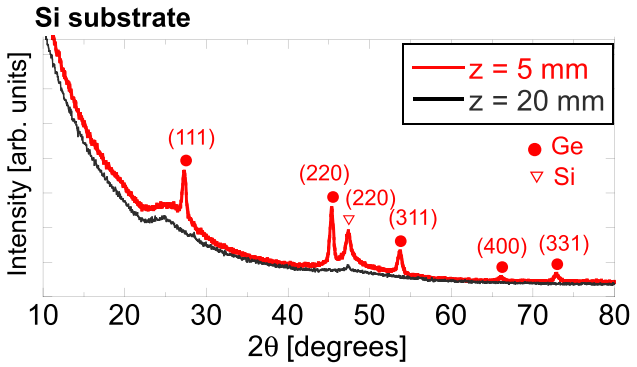


**FIGURE 4.** XRD patterns of Ge films deposited onto Si substrates at a target–substrate distance z of 5 mm and 20 mm and an RF input power of 60 W.

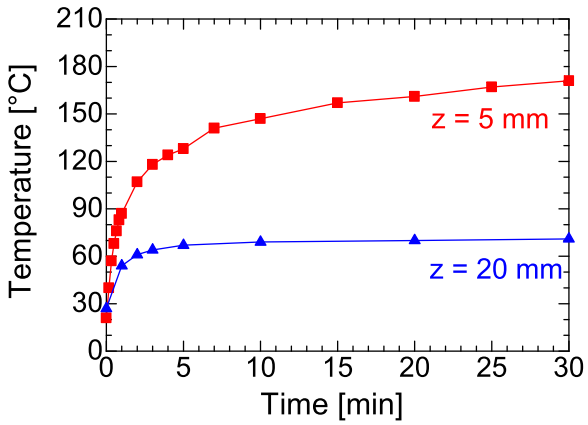


**FIGURE 5.** Time dependence of the thermocouple temperature at a target–substrate distance z of 5 mm and 20 mm and an RF input power of 60 W. The thermocouple sensor was positioned on the substrate.

0.5 Torr. As shown in Fig. 2(d), the size of the nanograins increased with decreasing z, and the average grain sizes for z = 5, 10, and 20 mm were 100, 57, and 48 nm, respectively. Here, the average size of the nanograins was estimated from the surface SEM by randomly selecting over 20 grains in the SEM image. This result is reasonable because the deposition rate of the Ge film markedly increased with decreasing z; the deposition rate for z = 20 mm was 90 nm/min, whereas that for z = 5 mm was as high as 660 nm/min. The shorter target–substrate distance leads to the larger amount of highly reactive Ge atoms impinging to the substrate surface, which results in the rapid growth of grains on the substrate and the high deposition rate. On the other hand, at high pressures such as 0.5 Torr, Ge nanoparticles could be synthesized in a gas-phase plasma because a higher-density plasma is produced locally in front of the cathode sputtering target [1], [14]. The shorter collision mean free path for Ge species would cause nucleation of nanograins in the gas phase [12], [15].

Fig. 3 shows Raman spectra of the Ge nanostructured films deposited at different z. Interestingly, we observed that the Ge structure markedly changes; the spectra of the films fabricated at z = 10, 20, and 30 mm show a broad peak at ∼270 $cm^{-1}$, which is assigned to Ge with an amorphous structure, whereas the spectrum of the z = 5 mm film shows a sharp peak at ∼300 $cm^{-1}$, which indicates the formation of crystalline Ge.

To confirm the structure inside the Ge nanograins in detail, XRD analyses were conducted (Fig. 4). The XRD patterns clearly show that the nanostructured film fabricated at z = 5 mm contains crystals with (111), (220), (311), (400), and (331) orientations. In the narrow-gap plasma sputtering in the sub-Torr range, nanocrystalline Ge films were fabricated at a high deposition rate without heating the substrate holder.

To analyze the mechanism of crystallization in the plasma sputtering process under the condition of a short target–substrate distance, the substrate surface temperature was roughly measured with a thermocouple probe, where the plasma and the neutral gas directly flowed to the small tip surface of the sensor placed on the substrate. As shown in Fig. 5, the thermocouple temperatures rapidly increased with increasing the deposition time until the deposition time reached 5 min (i.e., 70 °C at z = 20 mm and 170 °C at z = 5 mm) and then showed an almost constant value after 30 min. A shorter z position led to a higher temperature of the sensor tip, which is attributed to 1) increased heat transfer from the sputtering target at an RF input power of 11.8 $W/cm^2$ through the flowing Ar gas and 2) an increase in the physical and chemical reactions by impinging ions from plasma on the surface [15]. The increased temperature explains the nanocrystal Ge formation in the z = 5 mm sample from a thermal viewpoint, although the melting point of bulk Ge is as high as 938 °C. In general, the melting point of nanoparticles is expected to decrease with decreasing particle size [16]. The lower melting point related to nanosized particles and a thin layer might play important roles in the crystallization of nanostructured Ge films at low temperatures.

Fig. 6(a) and (b)–(d) show Raman spectra and surface SEM images, respectively, of films deposited at different RF input

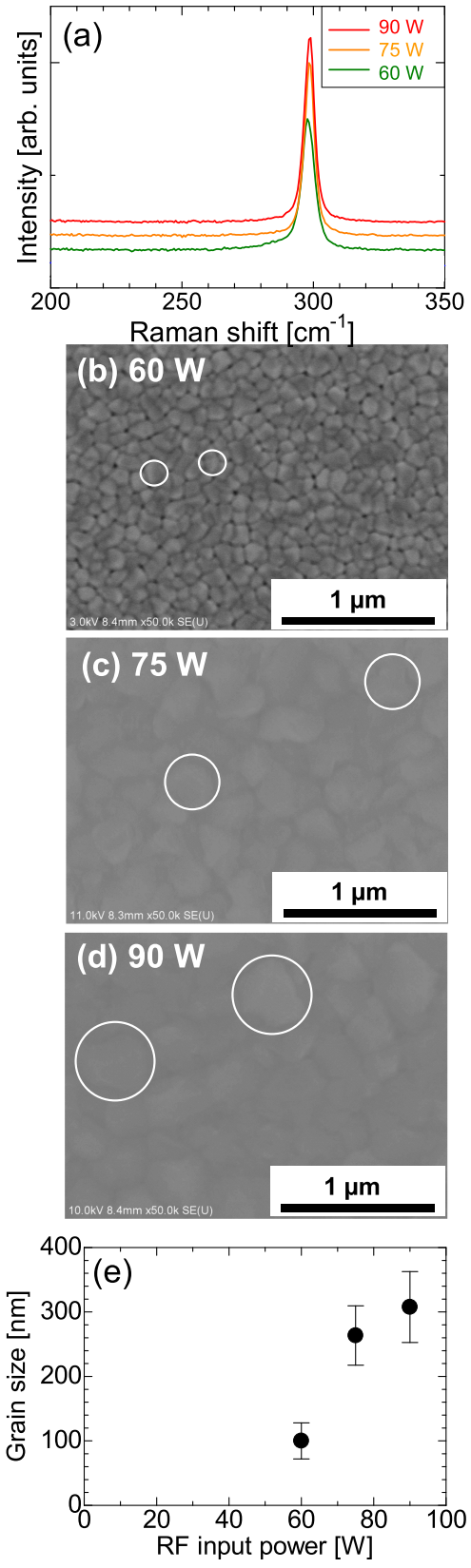


**FIGURE 6.** **(a) Raman spectrum of Ge films deposited onto Si substrates at a target–substrate distance of 5 mm and an RF input power of 60 W, 75 W, and 90 W. SEM surface images of Ge films deposited at a target–Si substrate distance of 5 mm and an RF input power of (b) 60 W, (c) 75 W, and (d) 90 W. (e) Dependence of the grain size on an RF input power.**

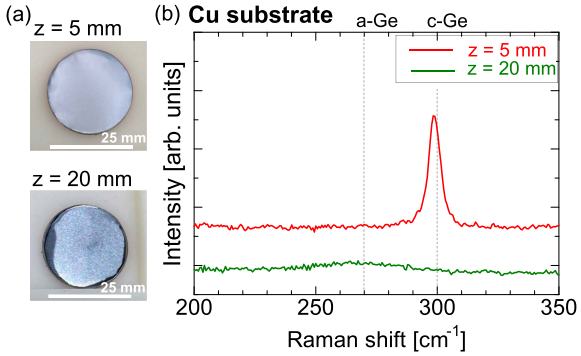


**FIGURE 7.** **(a) Film surface images and (b) Raman spectrum of Ge films deposited onto Cu substrates at a target–substrate distance z of 5 mm and 20 mm and at an RF input power of 60 W.**

powers for plasma production, where all the Si substrates were positioned at z = 5 mm. The spectra of all the films show a sharp Raman peak at ~300 $cm^{-1}$, which is assigned to crystalline Ge. As shown in Fig. 6(b)–(d) (surface SEM images) and Fig. 6(e) (grain size measurement), the average size of nanograins increased from 100 to 263 and 307 nm when the RF input power was increased from 60 W (11.8 $W/cm^2$) to 75 W (14.8 $W/cm^2$) and 90 W (17.7 $W/cm^2$), respectively. The higher RF input power leads to a higher plasma density, to a higher deposition rate, and to a higher temperature of the grain surface, which would enhance nanocrystal growth both in the gas-phase plasma and on the substrate.

A nanocrystalline Ge film was subsequently deposited onto a thin Cu substrate to a thickness of 80 $\mu$m using the developed plasma sputtering method under a sub-Torr pressure of 0.5 Torr and small z of 5 mm. Fig. 7(a) and (b) show images of the Ge film surface and the Raman spectra, respectively, of Ge films deposited at z = 5 and 20 mm. Similar to the Raman spectra of Ge films on Si substrates, the Raman spectra of Ge films on Cu substrates show a transition from an amorphous to a crystalline structure as z is decreased from 20 to 5 mm, accompanied by a change in the color of the film surface from metallic to dark gray. We successfully fabricated nanocrystalline Ge films on a thin Cu substrate at high speed using sub-Torr and narrow-gap plasma sputtering.

To demonstrate the advantages of the plasma process for low-temperature nanocrystal formation, we fabricated crystalline Ge films using a thermal annealing process, which is the conventional method for inducing crystallization of a solid phase. Here, the amorphous Ge films were deposited by sputtering at z = 20 mm and subsequent thermal annealing at 300–500 °C under a $N_2$ atmosphere. Fig. 8(a) and (b) show the Raman spectra obtained for Ge films on Si and Cu substrates, respectively. For Ge films on Si substrates, the amorphous Ge layer crystallized at 500 °C, which is similar to the crystallization temperature reported in a previous study [10]. However, for the Ge film on a Cu substrate, Raman signals at 270 and 300 $cm^{-1}$, which are related to amorphous and crystalline structures, respectively, were not detected after the sample was annealed at 500 °C. Interestingly, the color of

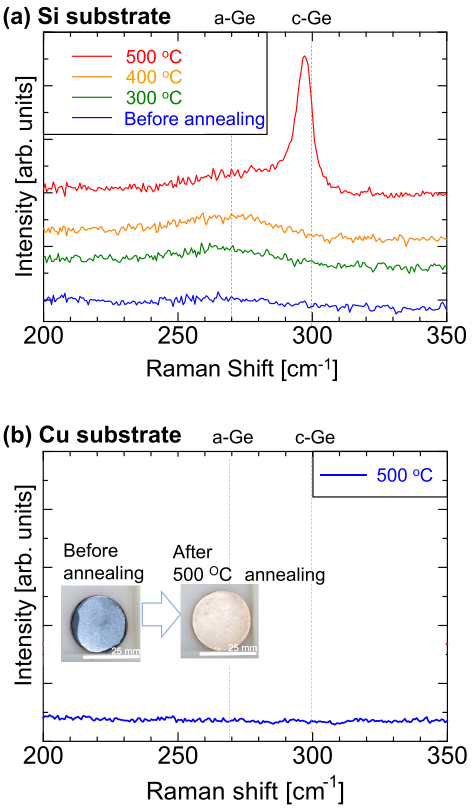


**FIGURE 8.** **(a) Raman spectrum of Ge films on Si substrates after the films were annealed at 300 °C, 400 °C, and 500 °C. (b) Raman spectrum of a Ge film on a Cu substrate after the film was annealed at 500 °C.**

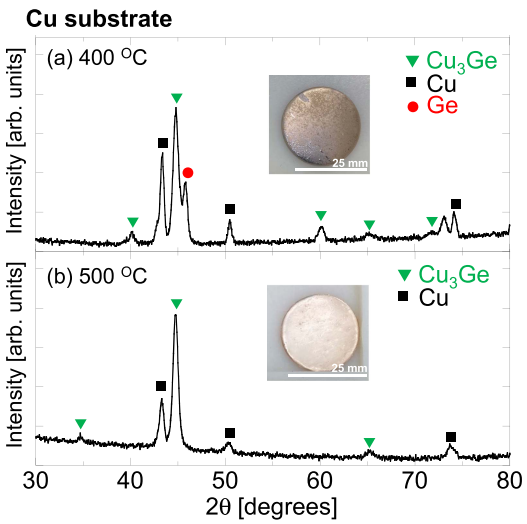


**FIGURE 9.** **XRD patterns of Ge films on Cu substrates after the films were annealed at (a) 400 °C and (b) 500 °C.**

the Ge film markedly changed after the annealing process at 500 °C (Fig. 8(b)). To identify the film structure, we analyzed the thermally annealed films by XRD. As shown in Fig. 9, peaks corresponding to Cu–Ge alloy were clearly observed in the patterns of films annealed at 400–500 °C [17], [18]. Previous studies have shown that annealing treatments at 400 °C are sufficient to induce complete crystallization of $Cu_3Ge$ films [19], [20], [21], [22], where the $Cu_3Ge$ stoichiometric compound is generated as a result of annealing-induced interdiffusion of Cu and Ge atoms. Via the same mechanism, the amorphous Ge layer on a thin Cu substrate could be converted to a $Cu_3Ge$ crystal layer by annealing at 400–500 °C under $N_2$. In the annealing process, a barrier layer between the Cu and Ge layers might be required to obtain a crystalline Ge film [10]. Our experiments show that the low-temperature plasma process is advantageous for the formation of a nanocrystalline Ge film via a simple single-step procedure. Electrochemical performance of Li ion batteries with the nanocrystalline Ge film on a Cu substrate will be tested in future.

In conclusion, we fabricated nanocrystalline Ge films with particle sizes of 100–307 nm by Ar plasma sputtering with a high Ar gas pressure of 0.5 Torr and a short target–substrate distance z of 5 mm, where the Ge films transformed from amorphous to crystalline with decreasing z. A nanocrystalline Ge film was successfully fabricated on a thin Cu substrate at high speed without heating the substrate; thus, the mixing of Ge and Cu atoms to form Ge–Cu alloy was prevented by the use of a low-temperature process. The formation of a nanocrystalline Ge film on various substrate materials was realized in a single-step procedure using low-temperature plasma.

## ACKNOWLEDGMENT

G. U. would like to thank Mr. Narishige and Prof. Itagaki (Kyushu University) for their AFM measurements.

## REFERENCES

[1] G. Uchida et al., "Nanostructured Ge and GeSn films by high-pressure He plasma sputtering for high-capacity Li ion battery anodes," *Sci. Rep.*, vol. 12, 2022, Art. no. 1742.

[2] D. Shahrjerdi et al., "High-efficiency thin-film InGaP/InAaAs/Ge tandem solar cells enabled by controlled spalling technology," *Appl. Phys. Lett.*, vol. 100, 2012, Art. no. 053901.

[3] S. Goriupatri, E. Miele, F. Angelis, E. Fabrizio, R. Zaccaria, and C. Capiglia, "Review on recent progress of nanostructured anode materials for Li-ion batteries," *J. Power Sources*, vol. 257, pp. 421–443, 2014.

[4] N. Nitta, F. Wu, J. Lee, and G. Yushin, "Li-ion battery materials: Present and future," *Mater. Today*, vol. 18, pp. 252–264, 2015.

[5] K. Toko, R. Numata, N. Oya, N. Fukuta, N. Usami, and T. Suemasu, "Low-temperature (180 °C) formation of large-grained Ge (111) thin film on insulator using accelerated metal-induced crystallization," *Appl. Phys. Lett.*, vol. 104, 2014, Art. no. 022106.

[6] K. Toko, R. Yoshimine, K. Moto, and T. Suemasu, "High-hole mobility polycrystalline Ge on an insulator formed by controlling precursor atomic density for solid-phase crystallization," *Sci. Rep.*, vol. 7, 2017, Art. no. 2460.

[7] S. Tanami et al., "Low temperature rapid formation of Au-induced crystalline Ge films using sputtering deposition," *Thin Solid Films*, vol. 641, pp. 59–64, 2017.

[8] N. Sunthornpan, K. Kimura, and K. Kyuno, "Crystallization of Ge thin films by Au-induced layer exchange: Effect of Au layer thickness on Ge crystal orientation," *Jpn. J. Appl. Phys.*, vol. 61, 2022, Art. no. SB1029.

[9] E. Stern, C. Bouldin, B. Roedern, and J. Azoulay, "Incipient amorphous-to-crystalline transition in Ge," *Phys. Rev. B*, vol. 27, pp. 6557–6560, 1983.

[10] C. Tsao, J. Weber, P. Cambell, P. Widenborg, D. Song, and M. Green, "Low-temperature growth of polycrystalline Ge thin film on glass by in situ deposition and ex situ solid-phase crystallization for photovoltaic applications," *Appl. Surf. Sci.*, vol. 255, pp. 7028–7035, 2009.

[11] G. Uchida et al., "Surface nitridation of silicon nano-particles using double multi-hollow discharge plasma CVD," *Phys. Status Solidi C*, vol. 8, pp. 3017–3020, 2011.
[12] M. Shiratani, K. Koga, S. Iwashita, G. Uchida, N. Itagaki, and K. Kamataki, "Nano-factories in plasma: Present status and outlook," *J. Phys. D: Appl. Phys.*, vol. 44, 2011, Art. no. 174038.
[13] G. Uchida et al., "Effect of nitridation of Si nanoparticles on the performance of quantum-dot sensitized solar cells," *Jpn. J. Appl. Phys.*, vol. 51, 2012, Art. no. 01AD01.
[14] J. Hayashi et al., "Morphological control of nanostructured Ge films in high Ar-gas-pressure plasma sputtering process for Li ion batteries," *Jpn. J. Appl. Phys.*, vol. 61, 2022, Art. no. SA1002.
[15] L. Mangolini and U. Kortzhagen, "Selective nanoparticle heating: Another form of nonequilibrium in dusty plasmas," *Phys. Rev. E*, vol. 79, 2009, Art. no. 026405.
[16] L. Li et al., "Crystallinity-controlled germanium nanowire arrays: Potential field emitters," *Adv. Funct. Mater*, vol. 18, pp. 1080–1088, 2008.
[17] A. Kazimirov, E. Erofeev, I. Fedin, V. Kagadei, and Y. Yurjev, "Low resistance $Cu_3Ge$ compounds formation by the low temperature treatment of Cu/Ge system in atomic hydrogen," *IOP. Ser.: Mater. Sci. Eng.*, vol. 135, 2016, Art. no. 012016.
[18] N. Gokon et al., "Phase change material of copper-germanium alloy as solar latent heat storage at high temperature," *Front. Energy Res.*, vol. 9, 2021, Art. no. 696213.
[19] L. Krusin-Elbaum and M. O. Aboelfothh, "Unusually low resistivity of copper germanide thin films formed at low temperatures," *Appl. Phys. Lett.*, vol. 58, pp. 1341–1343, 1991.
[20] M. A. Borek, S. Oktyabrsky, M. O. Aboelfotoh, and J. Narayan, "Low resistivity copper germanide on (100) Si for contacts and interconnections," *Appl. Phys. Lett.*, vol. 69, pp. 3560–3562, 1996.
[21] G. Guizzetti, F. Marabelli, P. Pellegrino, A. Sassella, and M. O. Aboelfotoh, "Optical response of $Cu_3Ge$ thin films," *J. Appl. Phys.*, vol. 79, pp. 8115–8117, 1996.
[22] F. Wu, W. Cai, J. Gao, Y. Loo, and N. Yao, "Nanoscale electrical properties of epitaxial $Cu_3Ge$ film," *Sci. Rep.*, vol. 6, 2016, Art. no. 28818.